

1978

# The use of Fourier analyzed square waves in the determination of the modulation transfer function of photographic materials

David Moffett

John Stanton

Follow this and additional works at: <http://scholarworks.rit.edu/theses>

---

## Recommended Citation

Moffett, David and Stanton, John, "The use of Fourier analyzed square waves in the determination of the modulation transfer function of photographic materials" (1978). Thesis. Rochester Institute of Technology. Accessed from

This Senior Project is brought to you for free and open access by the Thesis/Dissertation Collections at RIT Scholar Works. It has been accepted for inclusion in Theses by an authorized administrator of RIT Scholar Works. For more information, please contact [ritscholarworks@rit.edu](mailto:ritscholarworks@rit.edu).

THE USE OF FOURIER ANALYZED SQUARE  
WAVES IN THE DETERMINATION OF THE  
MODULATION TRANSFER FUNCTION OF  
PHOTOGRAPHIC MATERIALS

by

David Moffett and John Stanton

A thesis submitted in partial fulfillment of the requirements for  
the degree of Bachelor of Science in the School of Photographic  
Arts and Sciences in the College of Graphic Arts and Photography  
of the Rochester Institute of Technology

March 1978

Thesis advisor: M.F. Abouelata

8924696

TABLE OF CONTENTS

Introduction	pg 1
Theory	pg 3
Experimental	pg 14
Discussion	pg 21
Conclusions	pg 31
Appendix	pg 34

## LIST OF FIGURES

1. MTF - Typical and the Ideal pg 3
2. Cascading MTF Curves pg 4
3. Application of MTF Curves pg 5
4. Sinusoidally Varying Transmission Distribution pg 7
5. Transmission Distribution of a Symmetrical Square Wave pg 10
6. Transmission Distribution of a Symmetrical Square Wave and Its First Harmonic pg 12
7. Master Square Wave Target pg 20
8. MTF - Conventional and Square Wave Methods pg 27a
9. Characteristic Curve - Kodak Fine Grain Aerial Duplicating Film Type 2430 pg 35
10. Characteristic Curve - Rochester Film Co. Type 3T Reversal Microfilm pg 36
11. Characteristic Curve - Rochester Film Co. Type 1K Microfilm pg 37
12. Characteristic Curve - Intermediate Square Wave Target pg 38
13. Characteristic Curve - Final Square Wave Target pg 39
14. Microdensitometer Calibration Curve - Sinusoidal Target pg 40
15. Microdensitometer Calibration Curve - Sinusoidal Sample pg 41

LIST OF FIGURES, CONT.

16. Microdensitometer Calibration Curve -  
Square Wave Target pg 42
17. Microdensitometer Calibration Curve -  
Square Sample pg 43
18. Conventional MTF - Target imaged at 1X  
reduction with no mask pg 44
19. Conventional MTF - Target imaged at 4X  
reduction with no mask pg 45
20. Conventional MTF - Target imaged at 4X  
reduction with mask pg 46

## LIST OF TABLES

1. A Typical Set of Frequencies Used to Determine MTF pg 9
2. Square Wave Frequencies and Their Harmonics pg 13
3. Frequencies of Sinusoidal Target pg 14
4. Computer Output Sample pg 24
5. Frequencies of Sample with Harmonics pg 26
6. Frequencies of the Square Wave Target and Sample pg 30
7. Processing Data for Figures 8 Through 20 pg 47
8. Equations of the Microdensitometer Calibration Curves pg 48

## ACKNOWLEDGEMENTS

A special thanks is extended to Professor Mohamed F. Abouelata for his patient help and inspiration throughout this project. Thanks also go to Todd Calvin and Russell Schuter of the Rochester Film Company, the faculty and staff of the Photographic Science department of RIT, and to Donald Brumbaugh of the RIT computer center.

## ABSTRACT

Fourier analysis and a computer were used to generate the Fourier series and coefficients for the transmission distribution of a square wave target and the effective exposure produced on Kodak Plus-X film. This was performed in an effort to find a workable alternative to the proposed American National Standards Institute (ANSI) method for the determination of the photographic modulation transfer function. The results showed that the square wave method generated a curve with the same general trend as the conventional ANSI method. The Fourier analyzed square wave method had a greater degree of variability than did the standard method. The square wave targets used for the determination were manufactured at the Rochester Institute of Technology.



## INTRODUCTION

The widespread acceptance of the modulation transfer function (MTF) as a means of describing the band limitations of photo-optical systems has raised interest in its determination. The American National Standards Institute has set forth a rigorous procedure for its determination. This method utilizes targets varying sinusoidally in transmission, over a range of frequencies. The modulation of the output distribution is divided by the input and plotted as a function of spatial frequency, which generates the MTF curve. This procedure is lengthy as compared to the square wave method which is the subject of this project.

Fourier mathematics, long used in the physical sciences, can be applied to the problem of MTF determination. Fourier mathematics breaks a periodic function such as a square wave, into an infinite set of harmonic components.

Incorporating the two aforementioned concepts, the photographic MTF of Kodak Plus-X film was determined. Both the conventional (sinusoidal) and square wave methods were used. The square wave MTF plot had the same general shape

as the conventional method but with a higher noise level. The eight square wave targets used were bar targets imaged onto film. The sinusoidal target used contained 19 frequencies. The proposed ANSI standard was followed or adapted to the square wave method. Due to apparatus restrictions, the tests were aimed at the lower frequencies (0 to 40 cycles per mm).

## THEORY

The modulation transfer function (MTF) is a quantitative and graphical description of the performance of an optical and/or imaging system over a range of spatial frequencies. The MTF is a useful measure of the effects of light scatter and absorption within the emulsion during exposure and chemical dynamics of photographic development.

A perfect system would, if it existed, reproduce small as well as large subject areas with equal fidelity. Such a system would have a flat response at a level of 1.0 or at a modulation equal to 100%.

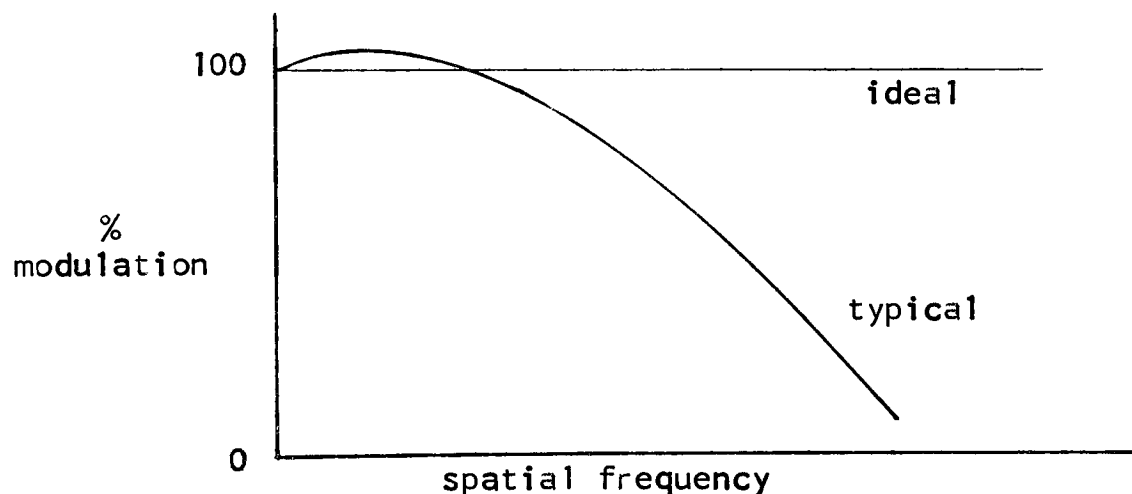


Figure 1. MTF - Typical and the Ideal

Since all physical systems are band limited and possess inherent noise, input signals are diminished or distorted. This results in a loss of image clarity and modulation. As the spatial frequency increases, the loss of modulation increases and clarity decreases.

Modulation transfer function curves are useful in selecting photographic materials and optical components for a number of professional applications. In a linear system, MTF curves can be cascaded so that a model can be visualized. This cascading is equivalent to point by point multiplication and is a useful approximation to the final system MTF.

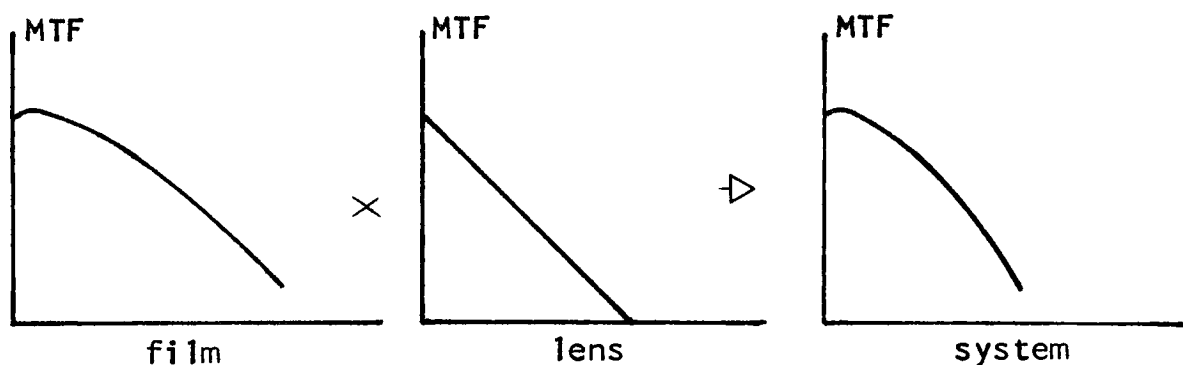


Figure 2. Cascading MTF Curves

Modulation transfer function curves can be utilized to select the best material for a job if the frequency range needed is known. This capability surpasses resolving power which only establishes an upper limit of frequency. In other words, MTF describes the material's ability to reproduce a range of frequencies.

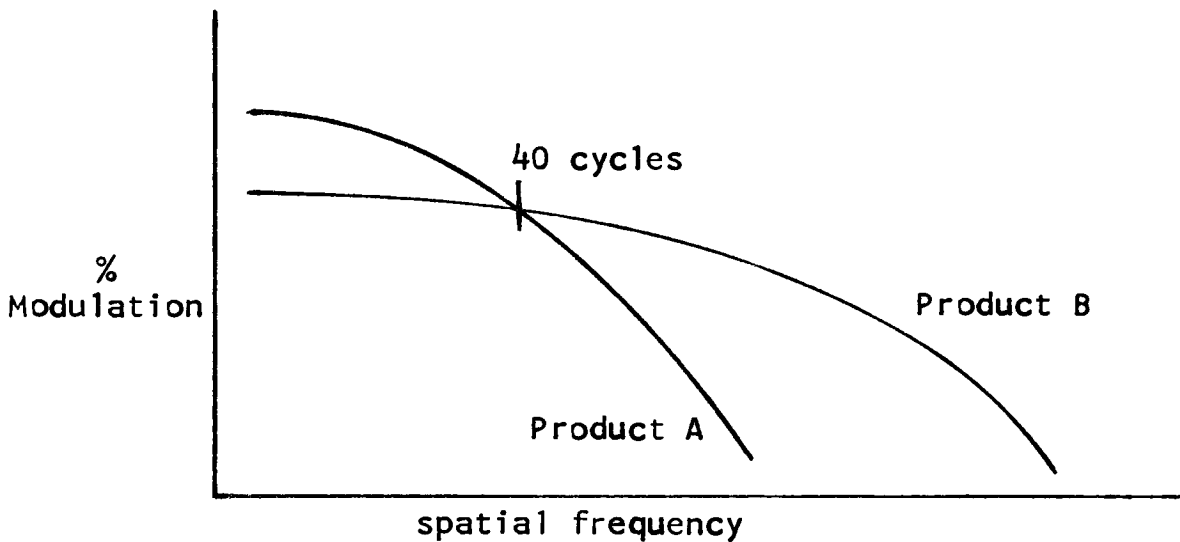


Figure 3. Application of MTF Curves

Referring to Figure 3, product A will reproduce spatial frequencies from 0 to 40 cycles/mm with more accuracy than

product B. Product B on the other hand, is capable of imaging objects of greater frequency than 40 cycles/mm with increased clarity over product A.

Modulation Transfer Function curves, or curves describing frequency response, have long been used as an index of band limitation. Amplifiers and other electrical devices are described and specified in terms of frequency. Since all physical systems have basic aforementioned similarities, Lamberts, Nelson, and Perrin<sup>1</sup> applied the concepts of frequency response to photo-optical systems.

In photo-optical applications, modulation describes the illumination or transmission differences of the source or target as a function of spatial frequency. The MTF is determined by dividing the output or effective exposure modulation by the input or incident exposure modulation at specific frequencies. These values are plotted versus frequency over a range to yield the MTF curve.

The input and output modulations are obtained from the transmission distributions of the target and image respectively. In the case of the sinusoidal target, the distribution is of the form in figure 4.

---

1. Kodak Technical Pamphlet, P-315, Kodak Plates and Films for Scientific Photography

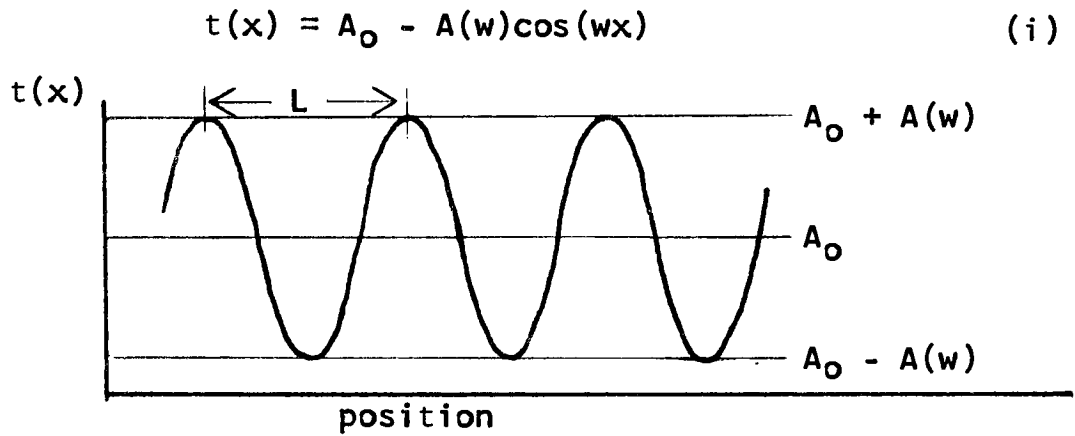


Figure 4. Sinusoidally Varying Transmission Distribution

The transmission distributions of the targets and the resulting images are obtained by microdensitometer scanning. The scanning generates a specular density versus position plot. The input exposure distribution is obtained by converting the specular density values to diffuse values. Conversion is possible using a calibration curve obtained by scanning uniform density patches with the microdensitometer and plotting specular versus diffuse density. The diffuse density values are then converted to transmission by the mathematical equation:

$$\text{transmission} = 1/10^{\text{density}} \quad (ii)$$

These values are then subtracted from the incident exposure to yield the input exposure distribution.

The output or effective exposure distribution is obtained in a similar manner. The target is imaged adjacent to a step wedge. The wedge is then scanned with the microdensitometer along with the target images. Reading the steps with a diffuse densitometer and plotting specular versus diffuse density generates the calibration curve. This is used to convert the specular densities of the target image to diffuse values. Using the D-Log H relationship, effective Log-H versus position is generated. The anti-log of the Log-H values are then plotted versus position to yield the effective exposure versus position curve.

Once the exposure distributions are obtained, modulation values for the input and output can be determined for each frequency. Output modulation divided by input modulation as a function of frequency is plotted to generate an MTF curve (see figure 1).

Reliable determination of the modulation transfer function is difficult for several reasons; band limitation of the equipment used, misalignment of optical components, and a large number of microdensitometer scans are needed, to name a few. The American National Standards Institute's proposed standard for the determination of MTF requires at



least thirteen frequencies ranging from 1.2 cycles/mm to 200 cycles/mm with an increment factor no greater than 1.6. Precision work often requires a minimum of twenty frequencies with at least ten cycles per frequency.

TABLE 1

A Typical Set of Frequencies Used to Determine MTF

1.2 c/mm	1.8	2.5
4.0	6.4	10.0
16.0	25.0	40.0
60.0	90.0	140.0
200.0		

The scanning and manipulating of these images is difficult and susceptible to error, both mechanical and human.

Fourier analysis is a method by which we can represent any periodic function as an infinite series of harmonic components. Cumulatively they are known as the Fourier series of the function. The chief prerequisite for obtaining the Fourier series of a function is that the function must be periodic. The period is the smallest distance with which the function repeats itself. Mathematically this is expressed by the equation:

$$f(x) = f(x + nL) \quad , \quad \text{where } n = \pm 1, 2, 3, \dots \quad (\text{iii})$$

L = the period

The complex Fourier series is written:

$$f(x) = \sum_{n=-\infty}^{\infty} c_n e^{inw_0 x} \quad (\text{iv})$$

where  $w_0$  = frequency in radians/mm

$$= 2\pi V_0$$

where  $V_0$  = frequency  
in cycles/mm

$$= 2\pi/L$$

The Fourier coefficients for the complex form are:

$$c_n = 1/L \int_{-\frac{1}{2}L}^{\frac{1}{2}L} f(x) e^{-inw_0 x} dx \quad (\text{v})$$

When  $n = 0$ , the level is obtained. When  $n = 1$ , the Fourier coefficient at the fundamental frequency is obtained.

Using  $n = 2$  yields the coefficient at the second harmonic, while setting  $n = 3, 4, \dots$  yields the coefficient at the third and fourth harmonics, and so on.

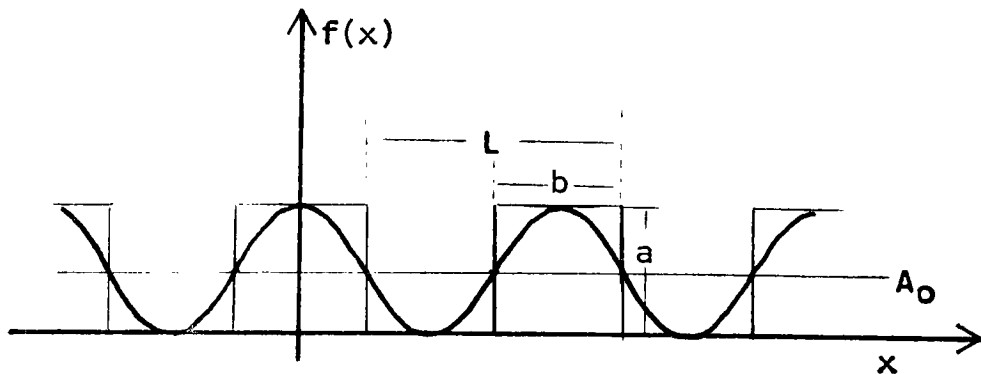


Figure 5. Transmission Distribution of a Symmetrical Square Wave

For the square wave in figure 5, the real form of the Fourier series is:

$$f(x) = \frac{A_0}{2} + \sum_{n=1}^{\infty} A_n \cos(n\omega_0 x) + B_n \sin(n\omega_0 x) \quad (\text{vi})$$

$$\text{where: } A_0 = 2C_0$$

$$A_n = C_n + C_n^* = 2(\text{real part of } C_n)$$

$$B_n = i(C_n - C_n^*) = -2(\text{imaginary part of } C_n)$$

For figure 5, the Fourier coefficients are:

$$C_n = \frac{ab}{L} \sin(nV_0 b) = \frac{ab}{L} \frac{\sin(\pi n V_0 b)}{\pi n V_0 b} \quad (\text{vii})$$

$$= \frac{a}{L \pi n V_0 b} \sin(\pi n V_0 b)$$

$$= \frac{a}{\pi n} \sin(\pi n V_0 b) \quad , \quad \text{since } L = \frac{1}{V_0}$$

$$= \frac{a}{\pi n} \sin\left(\pi \frac{n}{2}\right) \quad , \quad \text{since } b = \frac{L}{2} = \frac{V_0}{2}$$

Fourier series and transforms have been put to use in the electrical and mechanical engineering fields to solve a variety of problems. Because of the similarities among physical systems, the principles of Fourier mathematics can be adapted to photo-optical systems.

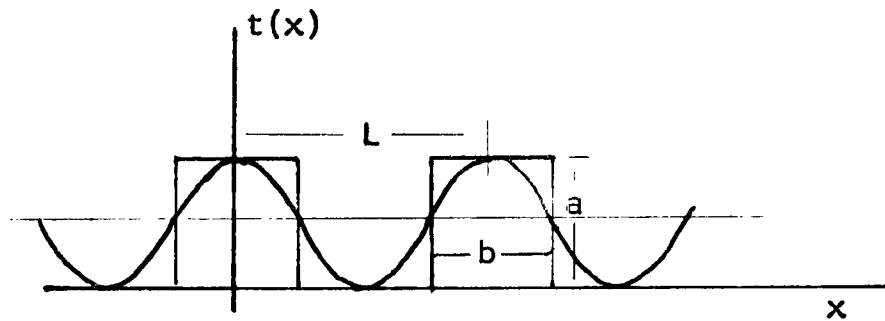


Figure 6. Transmission Distribution of a Symmetrical Square Wave and Its First Harmonic

Given a symmetrical square wave target, the MTF of an imaging system can be determined from the amplitude spectrum on the input target and the amplitude spectrum of the output image. The Fourier coefficients at each harmonic, divided by the level, will yield a modulation value and hence, a portion of the data point.

$$MTF_{(nw_0)} = \frac{|C_n'| / |C_0'|}{|C_n| / |C_0|}, \quad n = 1, 2, 3, \dots \quad (\text{viii})$$

The prime figures represent data from the output amplitude spectrum while the others refer to the input.

One Fourier analyzed square wave will yield a number of useful modulation values. Therefore, the total number of targets, exposures, developments, and microdensitometer scans required to compute the MTF is reduced (compared to the number of steps required to produce an MTF conventionally).

The proposed ANSI standard for MTF determination requires at least thirteen separate exposures. Using a square wave target and Fourier analysis, the necessary number of exposures is reduced with no loss of information, since at least three useable harmonics are present at each frequency.

Twenty-one data points can be obtained using the square wave frequencies in table 2. This set meets the criterion set forth by the proposed ANSI standard.

TABLE 2

Square Wave Frequencies and Their Harmonics

square wave target frequency	Fundamental $C_1$	Third $C_3$	Fifth $C_5$
0.5 cycles/mm	0.5	1.5	2.5
1.0	1.0	3.0	5.0
2.0	2.0	6.0	10.0
2.5	2.5	7.5	12.5
5.0	5.0	15.0	25.0
20.0	20.0	60.0	100.0
25.0	25.0	75.0	125.0
40.0	40.0	120.0	200.0

## EXPERIMENTAL

The actual lab work was divided into two sections. The determination of the MTF using the conventional sinusoidal method and the determination of the MTF via the square wave method. Work on both parts progressed simultaneously.

### MTF via the Conventional Method

The sinusoidal target used for this determination was obtained from the Photographic Science department at the Rochester Institute of Technology. It consisted of nineteen different frequencies ranging from 0.36 to 41.6 cycles/mm.

TABLE 3

Frequencies of Sinusoidal Target

0.36 cycles/mm	2.90	9.09	23.87
0.75	3.77	11.96	29.47
1.11	4.48	15.08	36.57
1.50	6.09	17.78	41.60
2.22	7.41	20.83	

---

The target was imaged onto Kodak Plus-X film, using a Polaroid MP-4 copy stand with a 4x5 Polaroid Land camera. The target was backlit using a Graphic Lite D5000 standard viewer. To produce the full range of frequencies desired (approximately 0.5 to 160.0 cycles/mm), the sinusoidal target was imaged with a magnification of 1.0 and 0.25. The Plus-X was then developed in Kodak D-76 for 6.75 minutes at 68° F in a hard rubber tank. The resulting images were scanned with the Ansco Model 4 Automatic Recording Densitometer. The traces were analyzed and the MTF was plotted from the data. The maximum frequency obtained with definite modulation was 36.36 cycles/mm. Since it was felt that higher frequencies should be possible, the Polaroid system was suspected of having a poor quality lens. Since the lens board mounting system made it difficult to substitute another lens, a Honeywell Pentax 35mm SLR with a 55mm lens was substituted for the 4x5 Land camera. The sinusoidal target was again imaged at 1.0 and 0.25 magnifications onto Kodak Plus-X 135 film. A through-focus series was performed at each magnification. The exposed film was developed in D-76 for the recommended time at 68° F. The exposures made at 0.25 magnification were useless because of heavy streaks and abrasions running through the film strip. However, the exposures made at 1.0 magnification were acceptable, so they were scanned. The maximum frequency obtained

was 30.73 cycles/mm. This value was also lower than what was reasonably expected of the system. The resolving power was measured in an effort to determine what factors could be responsible for the low frequency response. A through-focus test was performed on the MP-4 system with the Polaroid 4x5 camera head. A USAF resolving power target was imaged at a magnification of 1.0 onto Plus-X 4147 film. The resolving power of the system was found to be only 30 lines/mm. The system was then examined for sources of flare and a mask was incorporated into the apparatus to prevent stray light from the D5000 from affecting the exposure. Resolving power increased to 45 lines/mm with the use of the mask. Although this was a definite improvement, it was still not at a level suitable for high frequency reproduction. Since higher frequencies appeared to be difficult to image with the existing system, it was decided that only the frequencies obtained with the magnification of 1.0 would be used (table 3). The sinusoidal target was then masked, imaged onto Plus-X film using the Polaroid 4x5 camera head, and developed in D-76 for 7 minutes at 68° F. The resulting images were scanned on the microdensitometer, the traces analyzed, and the MTF plotted.



### MTF via the Square Wave Method

Several methods of manufacturing a suitable target were investigated. The first method involved the use of two Ronchi rulings, 1.97 and 3.94 cycles/mm. These rulings were imaged onto Kodak Aerial Film Type 2430 using the MP-4 stand with a Calumet 4x5 view camera, at a magnification of 1.0. The Polaroid camera was not available at this time. The film was processed in Kodak DK-50 for the recommended time at 68° F. The resulting images were mottled and of extremely poor quality. Variations in processing time, temperature, and agitation failed to improve image quality. From the procedures conducted, it was concluded that the film was defective due to poor storage. Kodak Contrast Process Pan Film Type 4155 was substituted for the 2430. The rulings were imaged again using the Polaroid 4x5 camera head. The film was processed in D-19 at 68° F. for 5 minutes. Although these images were of suitable quality, it proved difficult and time consuming to adjust magnification and exposure in order to obtain the eight targets desired.

A second method of manufacturing the square wave target involved the use of Chart-Pak tape affixed to a piece of white mounting board (Figure 7). Using two sizes of tape, 1/4 and 1/8th inch, made it possible to image two frequencies

simultaneously. This reduced the number of exposures needed for the end product. The master was imaged onto General Photo Products lithographic film at a 3x reduction using a Kenroe Vertical process camera. The film was processed in Kodalith chemistry. This system proved unsatisfactory because the maximum frequency reproduced was only 10 cycles/mm. The same procedure was then performed using a Robertson Process camera. Resolution increased to 30 cycles/mm. It was decided to use this system to manufacture targets of 0.5, 1.0, 2.0, 2.5, and 5.0 cycles/mm. An additional target with a frequency of 1.25 cycles/mm was also made. The 1.0, 1.25, and 2.0 cycles/mm targets were sent to Photographic Sciences Corporation where they were reduced 20x to yield targets with frequencies of 20, 25, and 40 cycles/mm. The contrast ratio of the images was approximately 1000:1. These eight targets were then mounted on a glass support to form the original square wave target. Since it was desired to have the contrast ratio of the square wave target equivalent to the contrast of the sinusoidal target, the original square wave target had to be duplicated onto a lower contrast material. In order to minimize harmonic distortion, a reversal process with a gamma of -1 was to be used. The original square wave target was contacted onto a sheet of Rochester Film Co. Type 3T reversal microfilm. It was then processed in Kodak D-19

for 5 and 12 minutes (first and second developer, respectively). Varying development times failed to lower the gamma appreciably. Kodak Plus-X type 4147 was then substituted for the 3T microfilm and processed according to an article by Arthur S. Beward<sup>2</sup>. Again, the gamma was too high and variations in processing failed to produce significant change. A two step contact process was substituted for the reversal system. The original square wave target was contacted onto Rochester Film Co. Type 1K microfilm which was then processed in D-19 for 5 minutes at 68<sup>o</sup> F. Gamma of the 1K intermediate was 2.09. The 1K intermediate was then contacted to a sheet of Kodak Plus-X Type 4147. The Plus-X was developed in D-76 for 4 1/2 minutes to yield a theoretical gamma of -0.48.

$$(-0.48)(2.09) = -1.00$$

The actual gamma for the Plus-X was -0.42. Hence, the final gamma for the target was -0.88. This last image is called the final square wave target. Its contrast ratio is approximately 10:1.

This square wave target was then imaged onto Plus-X type 4147 film using the MP-4 stand with the Polaroid head.

---

2. Beward, Arthur S., "Reversal Development of Black and White Films," RIT Photo Scientist, March 1971, Vol. 2, No. 2, pg 2

A mask was used with the square wave target as with the sinusoidal target. The exposed film was processed in D-76 at 68° F. The images were then scanned in the microdensitometer. The traces were digitized and the data entered into the computer. The actual calculation of the MTF is described in the discussion.

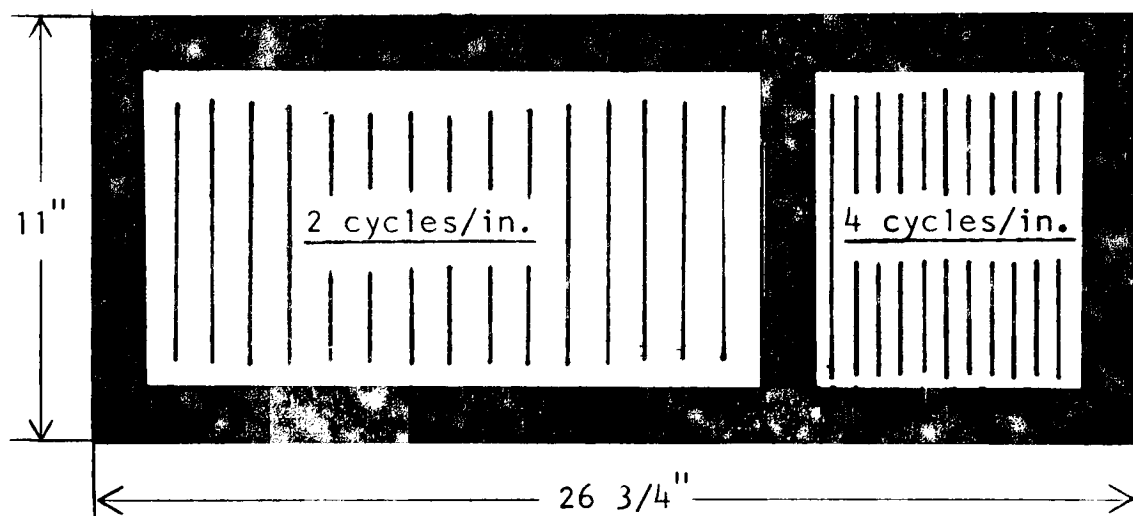


Figure 7. Master Square Wave Target

## DISCUSSION

This section will begin with a sample calculation of an MTF value determined by square wave analysis. Computation of the sinusoidally determined MTF is explained in the Theory section on page 6.

For this example, frequency patch #2 ( $V_0 = 2.011$  cycles/mm) will be used. First, the microdensitometer trace is examined. The frequency is calculated from a minimum of 10 cycles. The maximum and minimum values for specular density are then noted for the same 10 cycles. They are then averaged to yield one maximum and one minimum value. In this case:

### Specular density

$$\begin{aligned} D_{\max} &= 1.19 \\ D_{\min} &= 0.07 \end{aligned}$$

The next step is to "normalize" the trace to zero. Thus:

### Specular density

$$\begin{aligned} D_{\max} &= 1.12 \\ D_{\min} &= 0.00 \end{aligned}$$

The specular density is now converted to diffuse density via the equation:

$$D_{\text{diff}} = 0.751 (D_{\text{spec}}) + (3.61 \times 10^{-3})$$

$$= 0.850$$

Only the maximum value is used as this represents the height of the trace. The diffuse density is now converted to transmittance. According to the equation for the real form of the Fourier coefficients (equation vii), this will equal (a).

$$\text{transmittance} = a = 0.143 \quad (\text{xi})$$

Substituting 0.143 for (a) in equation (vii) yields the following values for  $C_n$ :

$\underline{n}$	$\underline{C_n}$
1	0.146
3	0.015
5	0.009

Again, from the real form:

$$C_0 = \text{level} = \frac{ab}{L}$$

$$= \frac{a}{2} \quad , \quad \text{since } b = \frac{L}{2} \text{ and } L = \frac{1}{V_0}$$

Thus:

$$C_0 = 0.059$$

From the theory, it is shown that the MTF as determined by the square wave method of analysis is calculated in the following manner:

$$MTF_{(nw_0)} = \frac{|C_n'| / |C_0'|}{|C_n| / |C_0|} .$$

Since the primed figures represent input values, the denominator refers to the square wave target. This portion is calculated first.

<u>HARMONIC</u>	<u> C<sub>n</sub>  /  C<sub>0</sub> </u>
1	0.639
3	0.208
5	0.125

The next step in the analysis is to examine the microdensitometer trace of the exposed images of the square wave target (the Plus-X samples). Again, 10 cycles were used to calculate the frequency of the patch. Three cycles were then chosen at random and specular densities read at equal position intervals for all three. The three readings at each position were averaged together to yield a single value. The result was a periodic set of data for

one cycle of the square wave at that particular frequency.

The computer program utilized in this project was obtained from the RIT-User's Computer Center library. It was written by John R. Merrill of Dartmouth College. In its original form, the program would generate its own set of data as the program was initially intended for instructional use only. The program was modified so that any periodic set of data could be used. From the data, the Fourier coefficients ( $A_n$ ) and ( $B_n$ ), and the value ( $A_0$ ) are computed (see equation vi). An example of the computer output for frequency patch #2 is shown in table 4.

TABLE 4

COMPUTER OUTPUT SAMPLE

$$A_0 = 0.774500$$

<u>HARMONIC</u>	<u>A</u>	<u>B</u>
1	3.90585E-02	-0.366492
3	-2.67930E-03	-4.60720E-02
5	-1.93645E-02	-2.41352E-03

From the derivation of the real forms of the Fourier series and coefficients, it is found that ( $C_n$ ) is related



to  $(A_n)$  and  $(B_n)$  in the following manner:

$$|C_n'| = \frac{1}{2} \sqrt{A_n^2 + B_n^2} \quad (\text{xiii})$$

Sustituting the numerical values from the computer output into equation (xiii) yields:

<u>HARMONIC</u>	<u> C<sub>n</sub>' </u>
1	0.185
3	0.023
5	0.010

The numerator of equation (viii) is now calculated.

<u>HARMONIC</u>	<u> C<sub>n</sub>'  /  C<sub>0</sub>' </u>
1	0.477
3	0.119
5	0.026

The numerator and denominator for equation (viii) have now been computed. The actual MTF value is now calculated.

<u>HARMONIC</u>	<u>MTF</u>	<u>FREQUENCY</u>
1	0.746	1.918 cycles/mm
3	0.570	5.754
5	0.208	9.590

The MTF values are then plotted versus the corresponding frequency. The total result is shown in figure 8.

Frequencies of the harmonics are calculated from the

frequencies of the patches on the sample. They are directly proportional to the fundamental:

<u>HARMONIC</u>	<u>FREQUENCY</u>
1	x
3	3x
5	5x

TABLE 5  
FREQUENCIES OF SAMPLE WITH HARMONICS

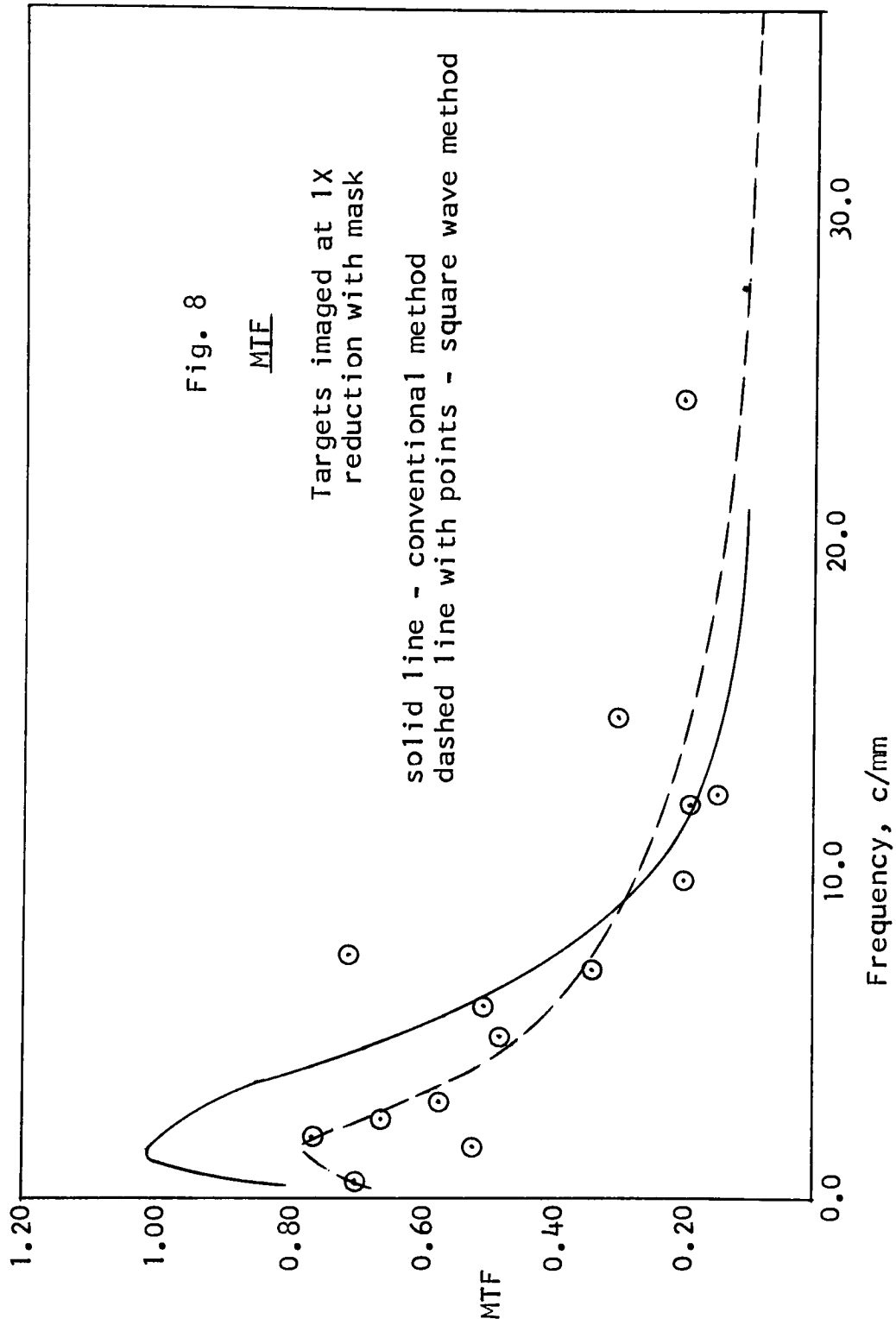
<u>Patch #</u>	<u>Harmonics</u>		
	1	3	5
1	0.488 c/mm	1.464	2.440
2	0.968	2.904	4.840
3	1.918	5.754	9.590
4	2.437	7.311	12.185
5	4.840	14.544	24.240
6	11.900	35.700	59.500

To simplify the explanation of the results, it is initially assumed that the MTF determined by the conventional sinusoidal method is correct for the system tested. The MTF obtained with the square wave method of analysis can

then be compared against this "correct" value for validity and accuracy.

The calculated MTF's for each method of determination are plotted in Figure 8. It can be seen that MTF measured by the square wave method yielded overall lower values for the lower frequencies (0 to 9 cycles/mm) as compared to those values obtained with the sinusoidal method. At frequencies higher than 9 cycles/mm, the two methods yielded MTF values that were approximately equal. The dashed line is a plot of the MTF determined by the square wave method - it has been drawn so as to smooth the trend of the actual points. The solid line represents the MTF determined conventionally. Both methods show a peak at approximately 1.5 cycles/mm, followed by a decrease for frequencies higher than 7 cycles/mm. As can be seen, there is a large amount of variability associated with the square wave MTF. In addition, there are two points (1.464 and 7.311 cycles/mm) which fall in areas seemingly unrelated to the general trend of the graph.

Differences between the output of the square wave method and the conventional method could be attributed to several possible sources of error. The first of these is the presence of harmonic distortion in the square wave



target. When manufacturing the target, a gamma equal to -1.0 was required to eliminate harmonic distortion. The actual product gamma on the square wave target was equal to -0.88, thus indicating the inevitable presence of distortion, although minimal. When calculating the MTF, harmonic distortion was assumed to be insignificant to simplify calculations.

Related to this are the computations involving the square wave target itself. Examination of the microdensitometer traces of the target showed that the lower frequencies (0.5 to 5 cycles/mm) approximated perfect square waves. The square wave target was therefore assumed perfect so that a simplified formula for computing the Fourier coefficients could be used. This would then totally ignore the mathematical considerations for any harmonic distortion that was present, not to mention degradation of edges and possible development effects.

Another plausible source of error was the Ansco microdensitometer used to scan the images. Once calibrated, it would give reliable readings. Unfortunately, due to a drifting circuit, re-calibration was required frequently. In addition, about midway through the analysis, repair work was performed on the instrument. At this time, the sinusoidal MTF had already been calculated while the square wave

method MTF analysis was just getting underway. Thus, it is possible that the adjustments made on the microdensitometer caused the MTF obtained by the square wave method to differ from that of the conventionally determined MTF. It is not conceivable however, that the microdensitometer was responsible for the relatively abnormal deviations in the MTF values for the square wave method.

In doing the calculations, a problem was encountered when the coefficients of the target were compared with the corresponding coefficients of the sample. After the target was made, it was scanned with the microdensitometer, and the frequency of each patch calculated. The target was then imaged at a 1.0 magnification onto Plus-X film. This was then scanned, and again, frequencies were computed for each patch. The target frequencies and the sample frequencies, however, weren't equal due to a magnification unequal to exactly 1.0. The differences are shown in table 6.

The frequencies used for figure 8 were the sample frequencies - frequencies of the harmonics were calculated from these (see table 5). The equations for calculating the MTF require that the input frequency be equal to that for the output frequency for that specific point. Although the differences are slight, they could be enough to produce a significant amount of variability.

TABLE 5  
FREQUENCIES OF THE SQUARE WAVE  
TARGET AND SAMPLE

<u>Cycles/mm</u>			
<u>Patch #</u>	<u>Target</u>	<u>Sample</u>	<u>Difference</u>
1	0.498	0.488	2.0%
2	2.011	1.918	4.6
3	1.004	0.968	3.6
4	2.514	2.437	3.1
5	5.000	4.848	3.0
6	12.387	11.900	3.9

Referring to figure 8, there are two points (1.464 and 7.311 cycles/mm) on the square wave method MTF curve which appear to bear no relation to the general trend of the graph. Both these frequencies are third harmonics derived from the 0.488 and 2.437 cycles/mm frequency patches respectively. There seems to be no obvious explanation for their behavior, as points derived from the same frequency patch for the first and fifth harmonics follow the general pattern set by the sinusoidally determined MTF.

## CONCLUSIONS

The results of this research, specifically the comparison of the MTF as determined by the two methods, can be briefly summarized with the following statements:

1. There was more variability associated with the square wave method of analysis.
2. Low frequency values (0 to 9 cycles/mm) generated with the square wave method were lower than those determined sinusoidally for the same frequency range.
3. High frequency values (9 to 20 cycles/mm) generated with the square wave method were slightly higher than those obtained conventionally over the same range of frequencies.
4. Both methods yielded curves with the same general trend.

While it is possible to name various sources of error as the causes for the first three statements, the fourth clearly indicates that MTF via a square wave method of analysis can be performed yielding results similar to a conventionally determined MTF of the same system. That

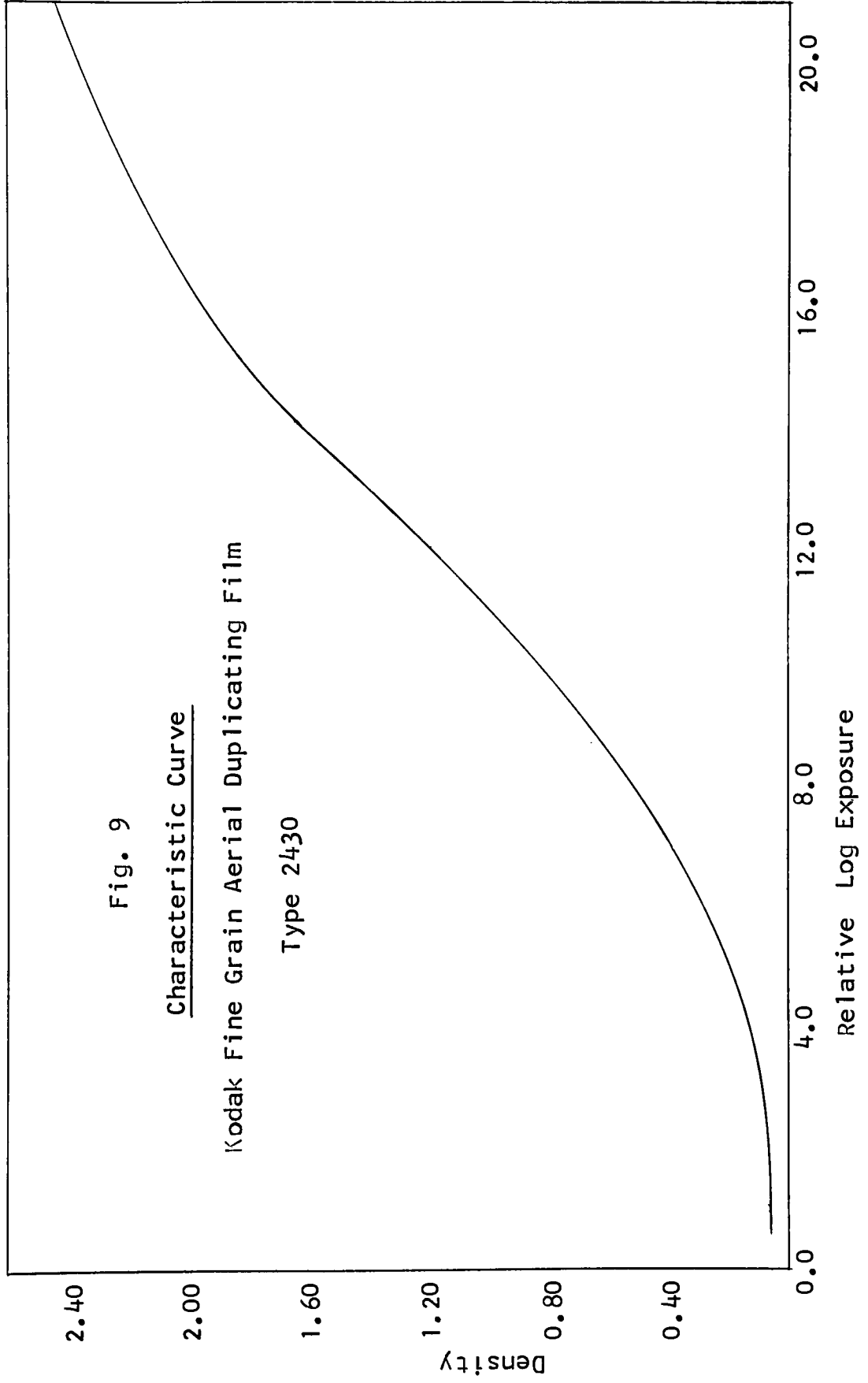


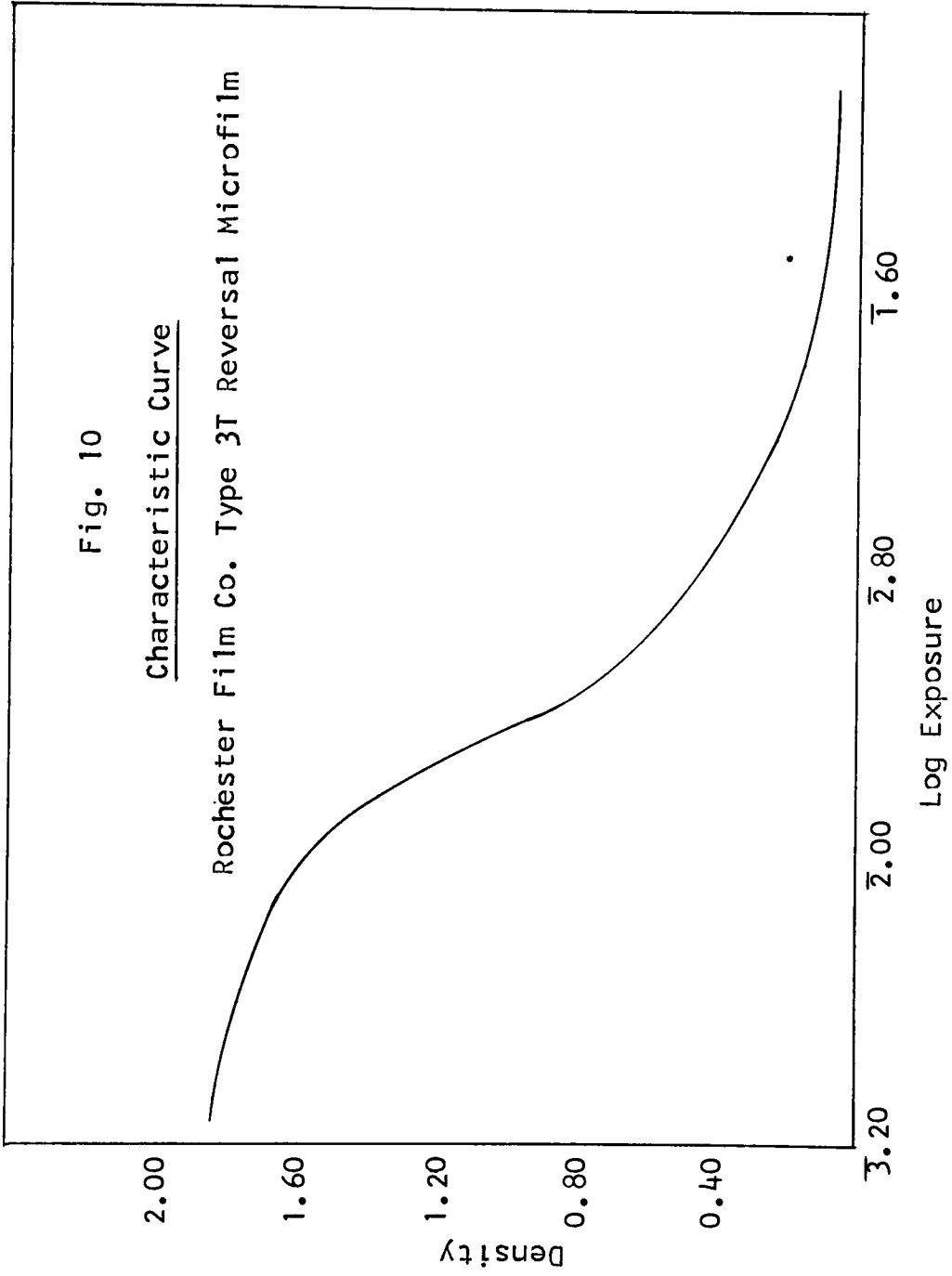
the shape of the two curves are relatively similar suggests that the square wave method can be used for an accurate MTF determination. Elimination of the sources of error described in the discussion could effectively reduce the amount of variability in the square wave method, thus making it a reliable measurement. The use of a high quality square wave target in a high resolution photo-optical system would no doubt be a first step in reducing the variability encountered in this project. The results of this experiment are only valid, of course, for the system that was used.

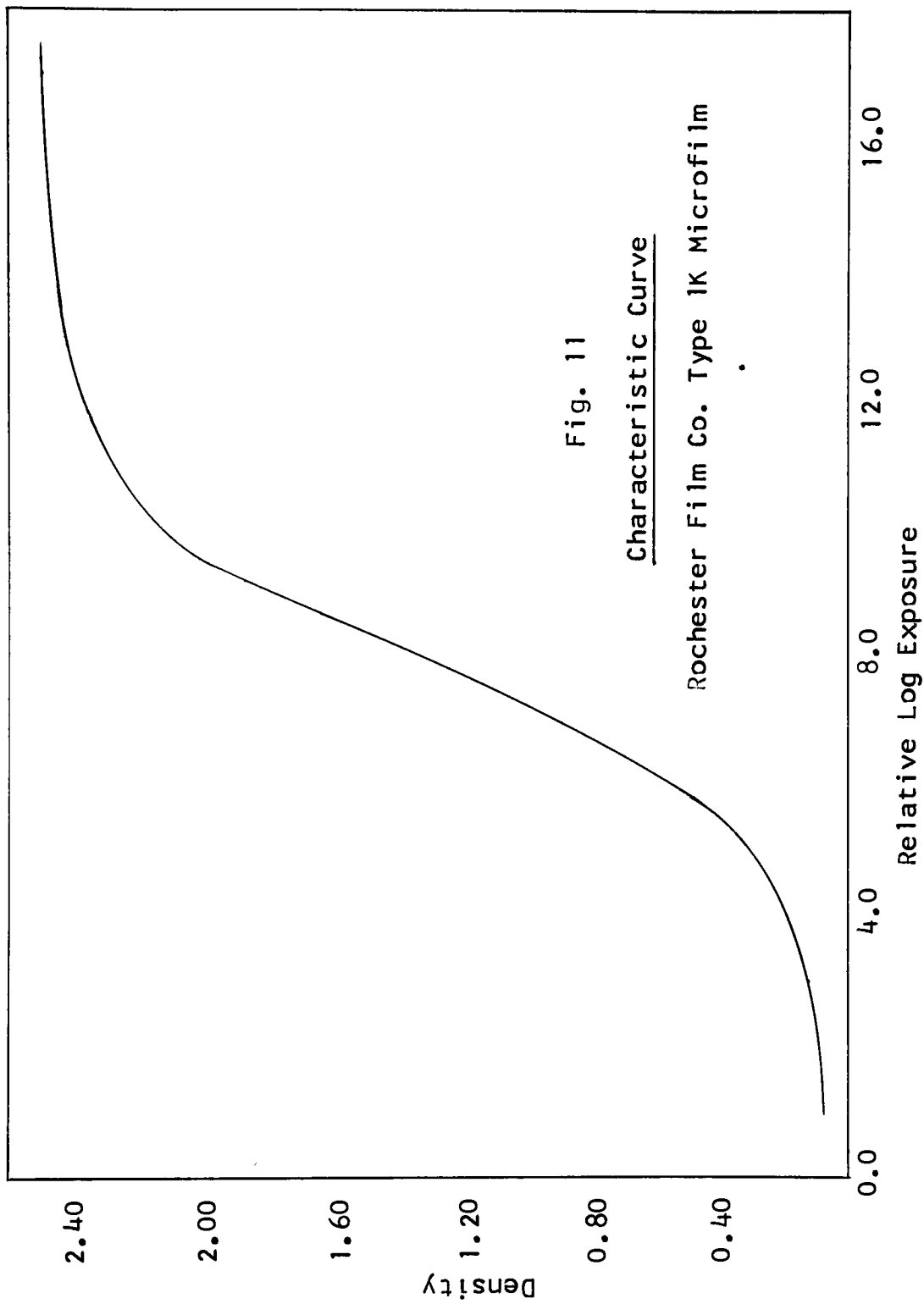
By using Fourier mathematics, the square wave is broken down into sinusoidal components (harmonics). The coefficients of these harmonics are then calculated and subsequently used to compute the MTF. Thus, several data points can be obtained from a single square wave frequency. In this project, only the first, third, and fifth harmonics were used. Three points were therefore calculated from one frequency imaged on the film, thus reducing the number of required targets (to obtain all of the required frequencies). In other words, MTF via square wave analysis using a high resolution photo-optical system would entail less work than an MTF determined sinusoidally and yet it would retain the same amount of accuracy.

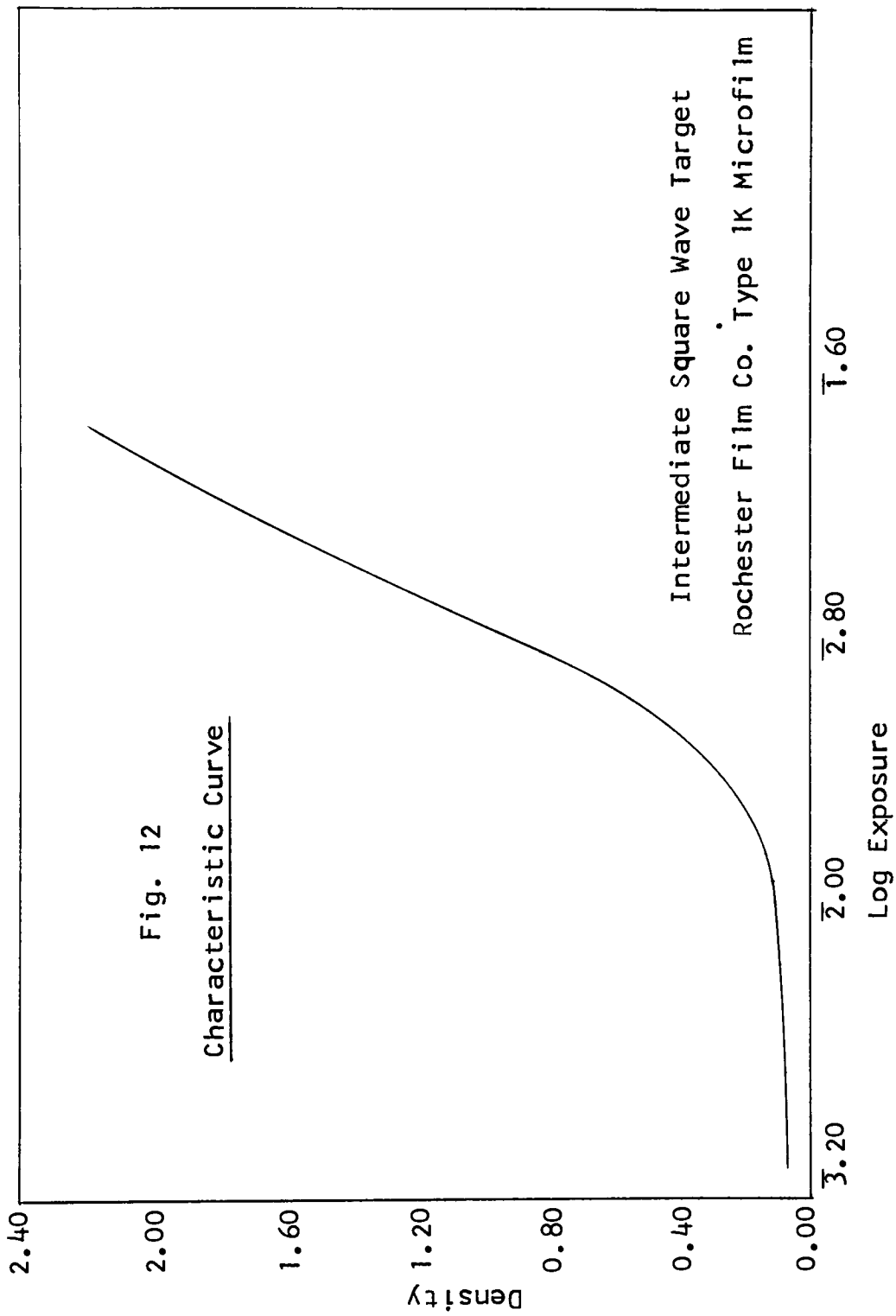
From the outcome of this analysis, it appears that the square wave method could be a feasible route for determining the MTF of a photo-optical system. Although a high degree of variability was encountered in the output of the square wave method, it clearly showed that it followed the same pattern set by the conventionally determined MTF.

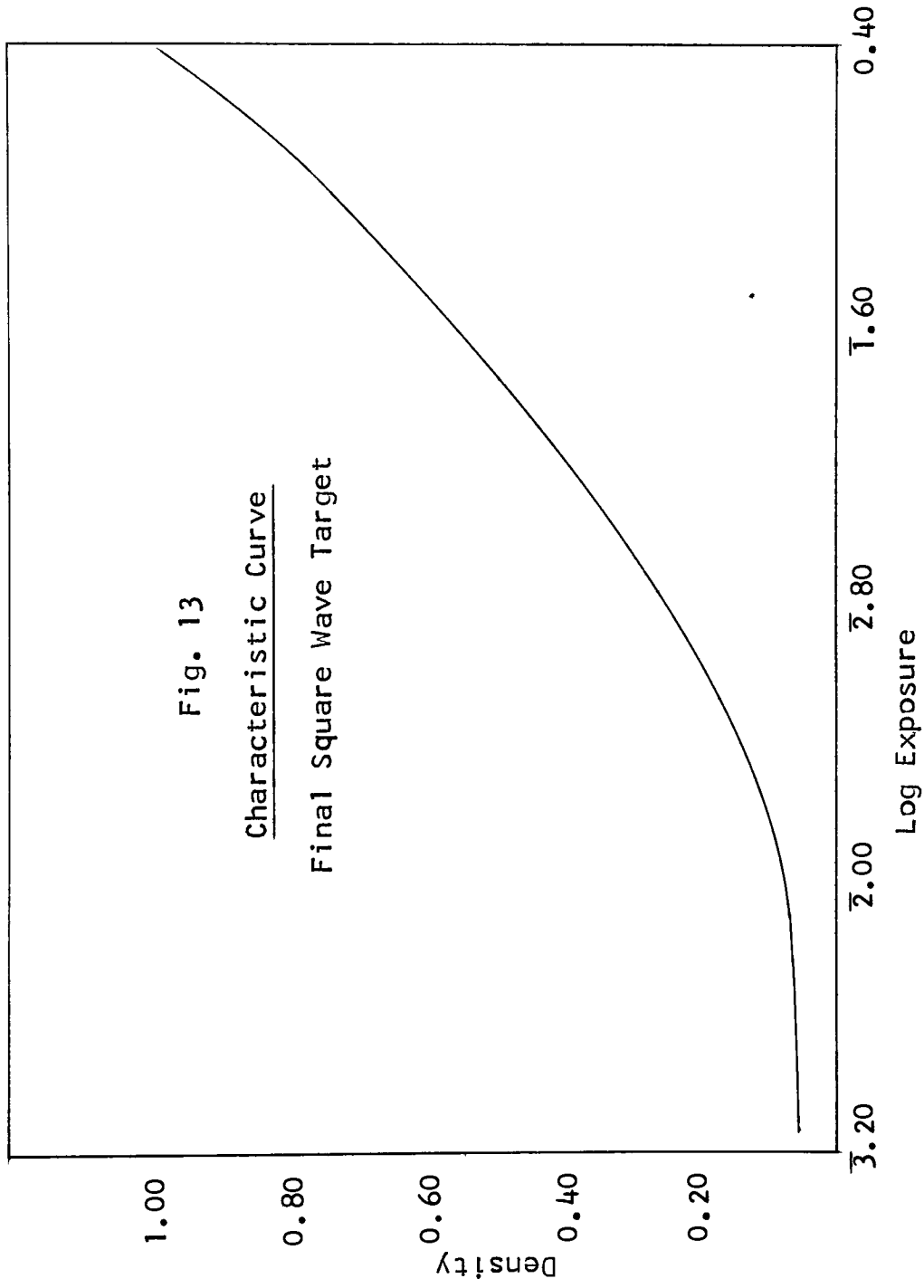
APPENDIX





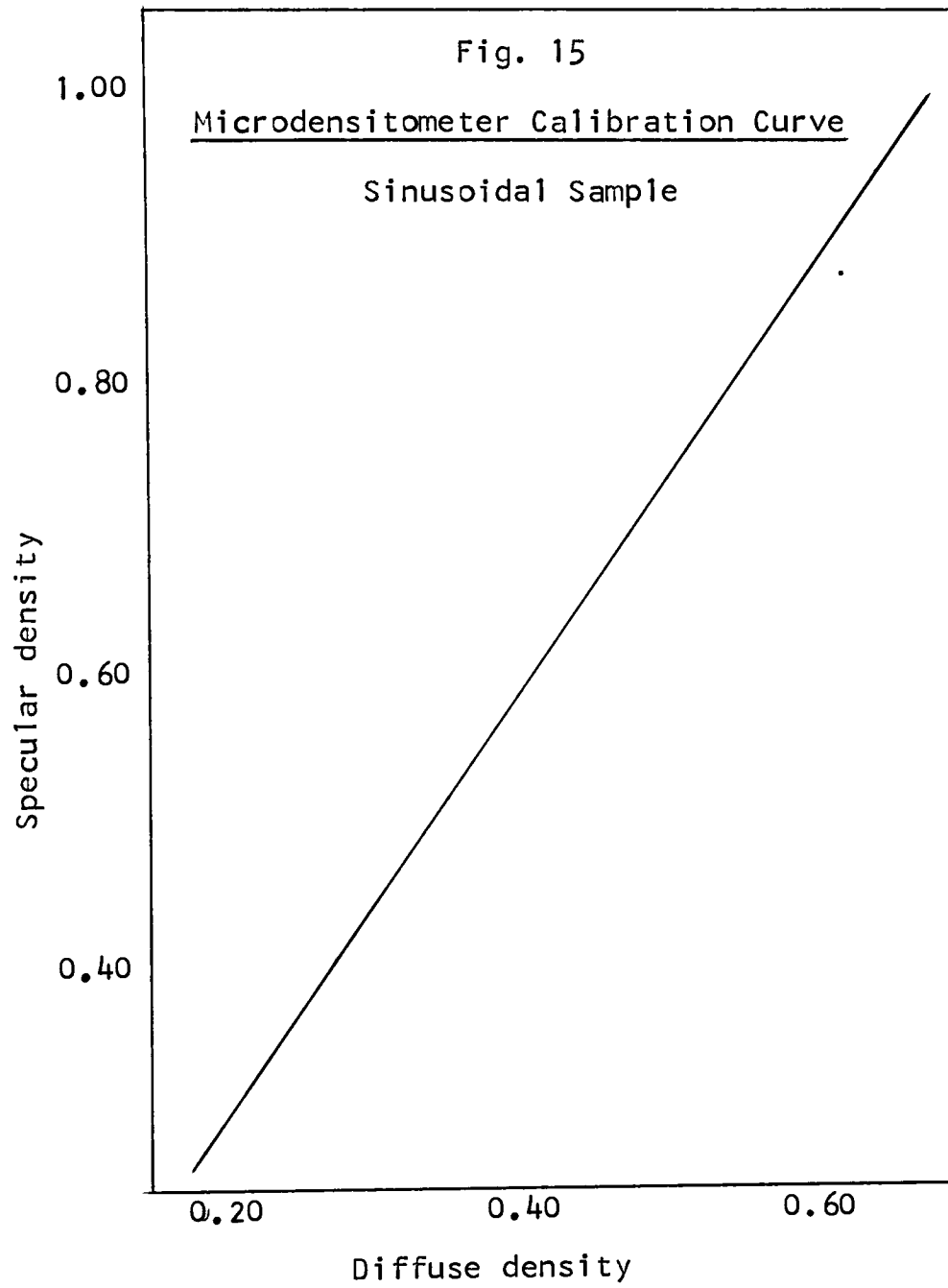


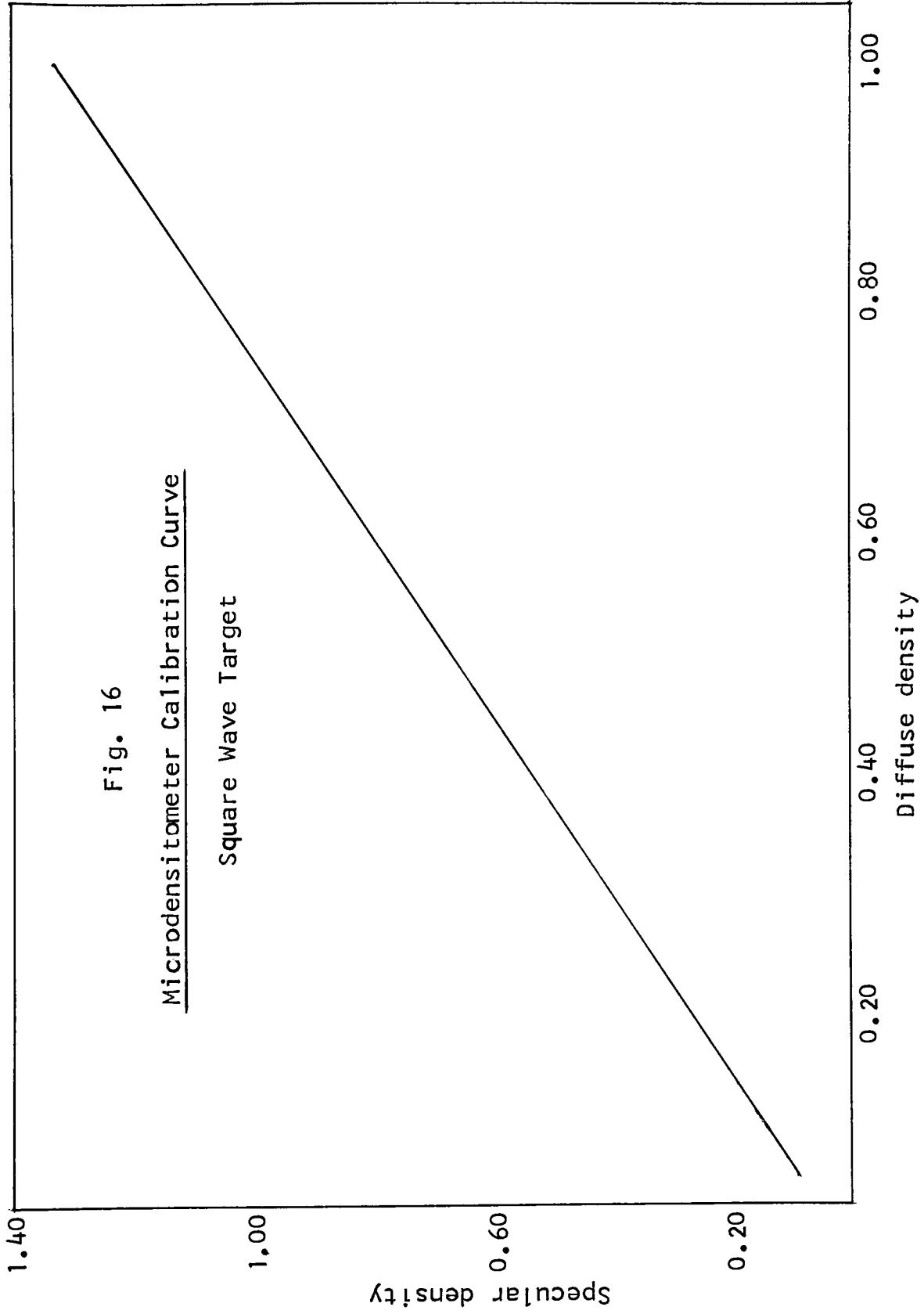


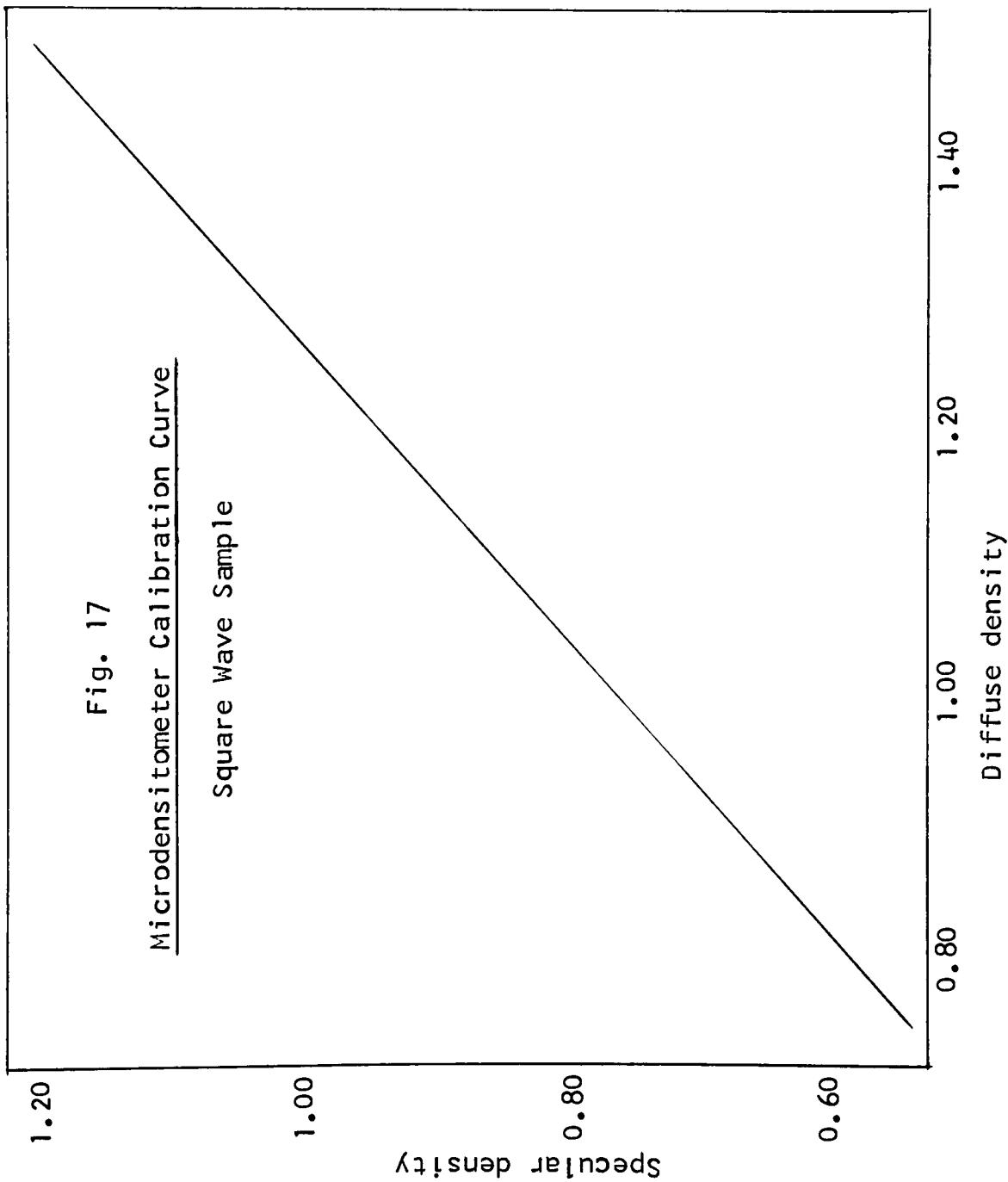


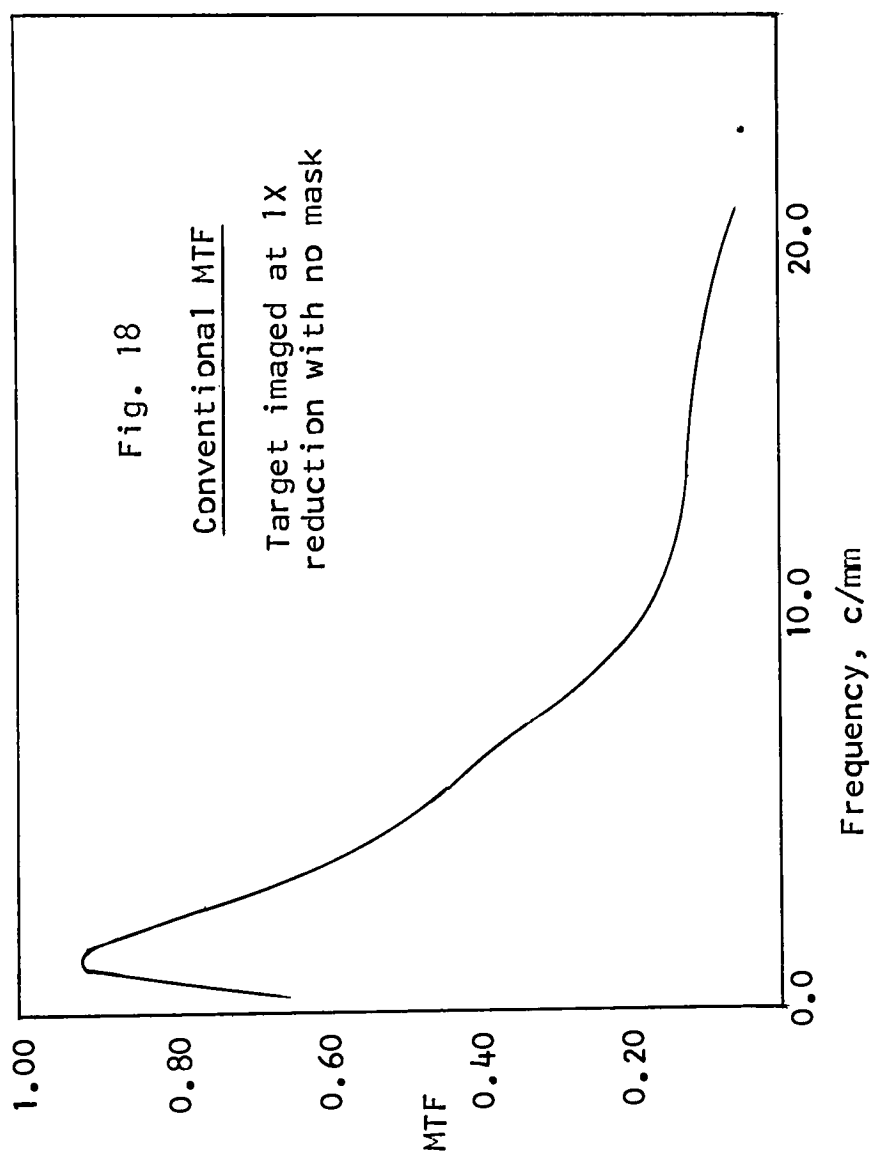


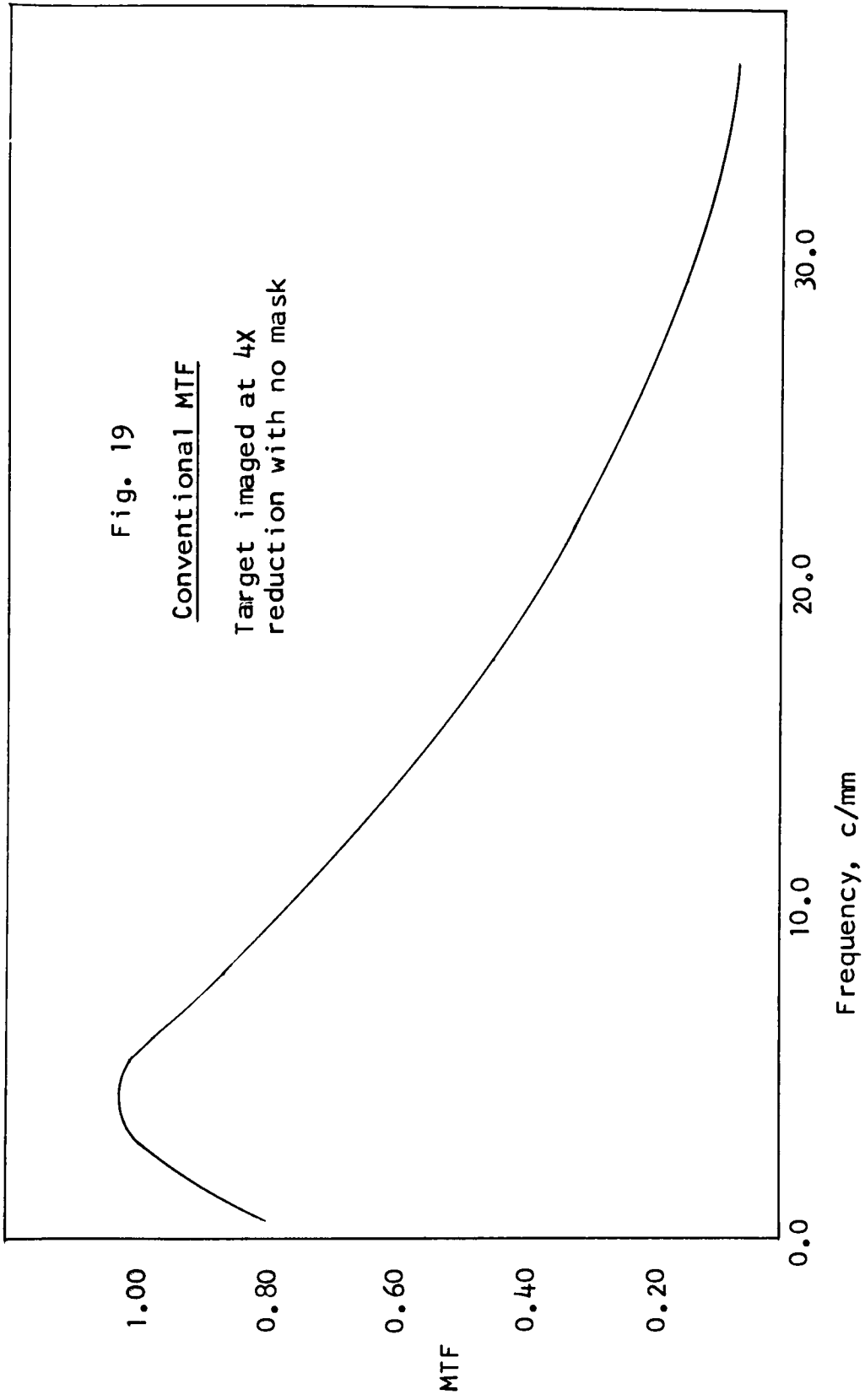












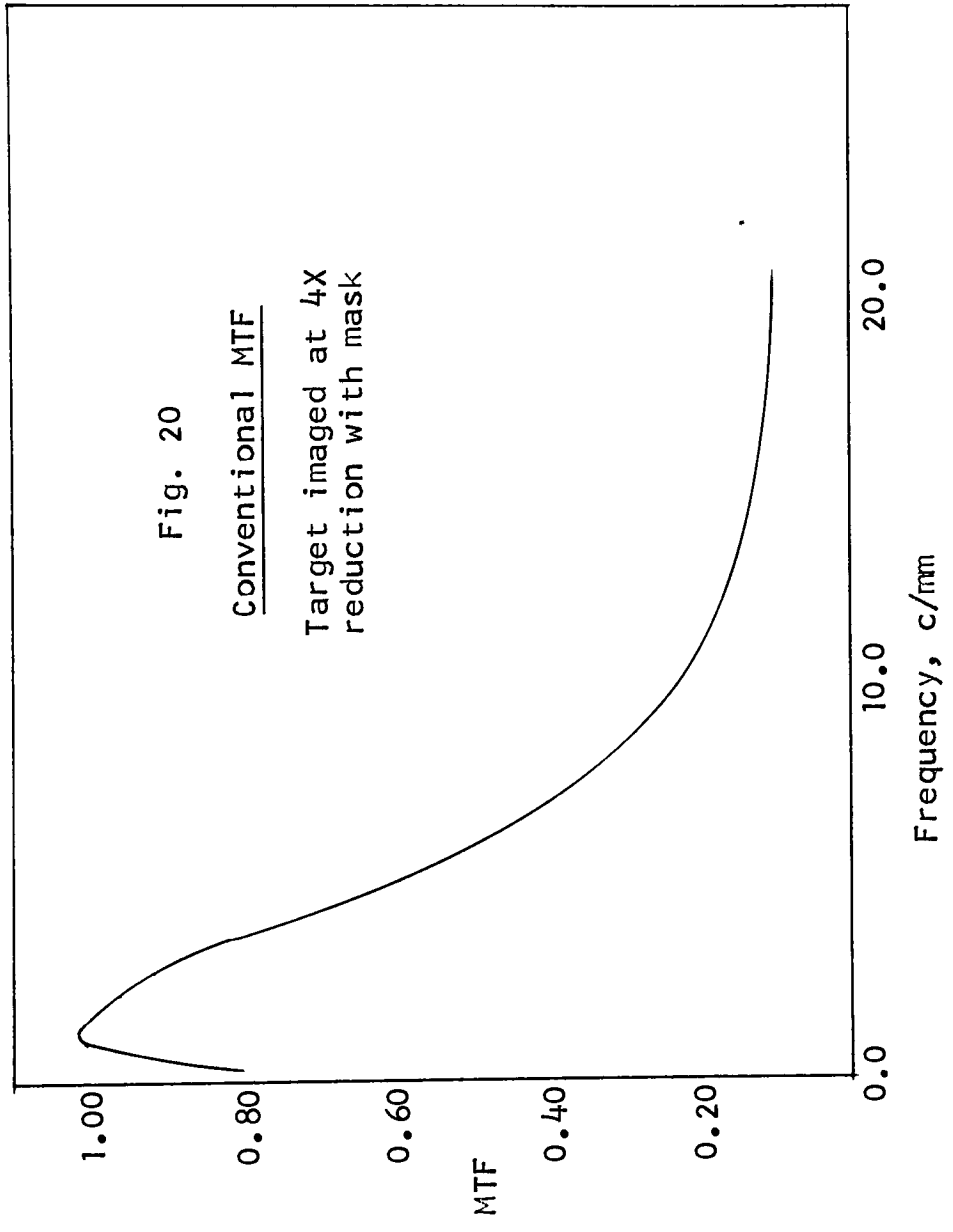


TABLE 7  
PROCESSING DATA FOR FIGURES  
8 THROUGH 20

8. Kodak Plus-X Type 4147, developed in D-76 at 68° F for 7 minutes
9. Kodak Fine Grain Aerial Duplicating Film Type 2430, developed in DK-50 for 5 minutes at 68° F
10. Rochester Film Co. Type 3T Reversal Microfilm, developed in D-19 (2.53 g/l NaSCN added) for 12 and 5 minutes (1st and 2nd developer) at 68° F
11. Rochester Film Co. Type 1K Microfilm, developed in D-19 for 5 minutes at 68° F
12. Rochester Film Co. Type 1K Microfilm, developed in D-19 for 5 minutes at 68° F
13. Kodak Plus-X Type 4147, developed in D-76 for 4 1/2 minutes at 68° F
14. no processing involved
15. Kodak Plus-X Type 4147, developed in D-76 for 7 minutes at 68° F
16. Kodak Plus-X Type 4147, developed in D-76 for 4 1/2 minutes, at 68° F
17. Kodak Plus-X Type 4147, developed in D-76 for 7 minutes at 68° F
18. Kodak Plus-X Type 4147, developed in D-76 for 7 minutes at 68° F
19. Kodak Plus-x Type 4147, developed in D-76 for 7 minutes at 68° F
20. Kodak Plus-X Type 4147, developed in D-76 for 7 minutes at 68° F



TABLE 8  
EQUATIONS OF  
MICRODENSITOMETER CALIBRATION CURVES

<u>Figure</u>	<u>Equation</u>
14.	$D_{\text{spec}} = 1.200 D_{\text{diff}} + 0.110$ $r^2 = 0.998$
15.	$D_{\text{spec}} = 1.424 D_{\text{diff}} + 0.014$ $r^2 = 0.996$
16.	$D_{\text{spec}} = 1.331 D_{\text{diff}} - (3.61 \times 10^{-3})$ $r^2 = 0.999$
17.	$D_{\text{spec}} = 0.885 D_{\text{diff}} - 0.100$ $r^2 = 0.999$

Note: All microdensitometer scans were made with a 10x/10x eyepiece/objective combination.

### GENERAL REFERENCES

1. Kodak Technical Pamphlet, M-61, Kodak Aerial Films and Photographic Plates
2. Kodak Data Book, P-52, Techniques of Microphotography - Precision Photography at Extended Reductions
3. Spiegel, Murray R., Mathematical Handbook of Formulas and Tables, Schaum's Outline Series
4. Sturge, John M., editor, Neblette's Handbook of Photography and Reprography, Chapter 9, "The Microstructure of the Photographic Image," by M. Abouelata, pg 197
5. Shaw, Rodney, editor, Selected Readings in Image Evaluation, Waverly Press Inc., 1976, Section 2